Materials Science-Poland, Vol. 24, No. 2/1, 2006

Carburisation of Fe–Ni–Cr alloys at high temperatures

A. UL-HAMID[1*], H. M. TAWANCY[1], S. S. AL-JAROUDI[2],
A. I. MOHAMMED[1], N. M. ABBAS[1]

[1]Center for Engineering Research, Research Institute,
King Fahd University of Petroleum and Minerals, P. O. Box 1073, Saudi Arabia

[2]Saudi Aramco, Tanajib, P.O. Box 65, Saudi Arabia

A large number of radiant tubes belonging to an ethylene furnace of a petrochemical plant failed during service. All tubes exhibited severe carburisation, while some of them lost their structural integrity and sagged. The tube material was based on a Fe–Ni–Cr alloy system with three varying compositions. Scanning electron microscopy and energy dispersive X-ray spectroscopy were used to characterize the microstructure and elemental composition of the tube material. Microhardness was tested to determine their mechanical strength. Experimental results indicated that the sagged tubes exhibited a higher degree of carburisation as compared to other tubes. The microstructure of these tubes also revealed coarser Cr-carbide precipitation and a continuous carbide lattice at austenite grain boundaries. It was concluded that exposure to excessive temperature during service was responsible for the degradation of all tube materials. Based on the above results, it is recommended that better control of furnace temperature should be employed in order to avoid overheating during service.

Key words: *Fe–Ni–Cr alloy; carburisation; SEM; furnace tube; high temperature*

1. Introduction

Ethylene (C_2H_4) is generated by cracking ethane (C_2H_6) in pyrolysis furnaces. The simplest illustration of the decomposition of ethane molecules into ethylene is represented by the following formula:

$$C_2H_6 \rightarrow C_2H_4 + H_2$$

The process stream in a furnace consists of a mixture of steam and ethane, passed through a coil of reaction tubes externally heated to the temperatures of 950–1150 °C. The temperature of the gas is raised quickly, and it is passed through

*Corresponding author, e-mail: anwar@kfupm.edu.sa

the coil at a high velocity with a short residence time. The temperature in the reaction tube is approximately 850 °C. It is well known that the process of producing ethylene generates free carbon according to the following reaction [1]:

$$C_2H_4 \rightarrow CH_4 + C$$

Carbon is deposited at the internal surface of the tube wall as adherent coke. The coke is removed by shutting off the hydrocarbon feed and passing air and steam through the coil. Such a process is known as decoking. Frequent decoking accelerates the thermal damage of the tubes, while less frequent decoking increases the rate of carburisation. The nominal and measured compositions of tubes made of three different alloys are shown in Table 1. Nine tubes, each with a wall thickness of approximately 8 mm, were examined in this study. The objective of this investigation was to compare the performance of furnace tubes, identify the cause(s) of their failure, and determine their suitability for service at high temperatures.

Table 1. Nominal and measured chemical compositions (wt. %) of tube materials

Element	Chemical composition (wt. %)					
	Nominal			Measured		
	Tubes					
	1, 2	3–6	7–9	1, 2	3–6	7–9
	HK-40(A351)	HP 25Cr-35 Ni, MA	35Cr-45 Ni, MA			
Ni	19–22	35	45	21.0	37.7	52.8
Cr	23–27	25	35	22.2	16.3	31.5
Si	1.75[a]	2.5	2.5	1.8	4.5	1.7
Fe	46.7–57.7	Bal.	Bal.	55.1	41.6	14.0
C	0.35–0.45	0.45	0.45	ND	ND	ND
Mn	1.5[a]	–	–	ND	ND	ND
Nb	–	1.5	1.5	ND	ND	ND
Other[b]	–	Ti, Zr	Ti, Zr	ND	ND	ND

[a]Maximum value.
[b]Small amounts.
ND – not detected in the tube alloy matrix.

2. Experimental procedure

The tubes were sectioned and mounted in cross-sections for metallurgical evaluation in both polished and etched conditions. The samples were etched with a freshly prepared mixture of 20 wt. % nitric acid (HNO_3) and 4 wt. % hydrofluoric acid (HF). The etchant was obtained by mixing 200 cm^3 of concentrated 70 wt. % HNO_3 with 70 cm^3 of concentrated 49 wt. % HF and 670 cm^3 of distilled water [2]. Each of the specimens was immersed in the etchant for two hours at room temperature and then rinsed with distilled water before drying. Microstructural features of the scale, the carburised zone, and the underlying alloy were characterized using a scanning elec-

tron microscope (SEM), and their chemical compositions were determined using energy dispersive X-ray spectroscopy (EDS). Vickers microhardness tests were used to compare the mechanical strength of the samples. The internal surfaces of the tubes were tested for carburisation using a NACE standard [2].

3. Experimental results

3.1. Visual inspection

Visual inspection revealed that sagging in four tubes (Nos. 3–6) resulted in a considerable loss of shape. Sagging was not observed in other tube samples. The scale formed on the surface of the tubes was adherent and there was no evidence of flaking. Effects of general or localized wall thinning were not observed in any of the tube samples. Moreover, no crackings in the tube walls were evident.

The stresses resulting from gas pressure in the ethylene production process are relatively low and it is well known that the most common failure modes of furnace components are longitudinal creep-rupture and carburisation [1].

3.2. Material verification

Elemental analysis of each tube sample was performed using energy dispersive X-ray spectroscopy. Representative EDS spectra and measured compositions for each tube material, along with its nominal composition, are shown in Figs. 1a–c and Table 1. The difference in composition between the nominal and measured values is expected due to the exposure of tube material to elevated temperatures in service. This exposure results in the precipitation of M-carbides (where M is Cr, Nb) within the matrix and at the grain boundaries, thus altering the starting composition of the matrix. Within this limitation, the measured composition can be seen to be in agreement with the nominal composition, confirming the tube materials are HK-40 (for tubes 1-2), HP 25Cr-35Ni Micro Alloy (for tubes 3-6), and 35Cr-45Ni Micro Alloy (for tubes 7-9). Based on the nominal composition, these alloys are suitable for the kind of service conditions encountered in an ethylene furnace. Alloy HK-40 is Ni-Cr grade, suitable for low stress reformer catalyst tube designs with service temperatures up to 1025 °C. Increased levels of silicon provide improved carburisation resistance, to benefit low severity ethylene cracking furnace coils. Alloy HP 25Cr-35Ni MA is a micro-alloyed HP with small additions of Ti and rare earth elements, which is especially stable at high temperatures. This alloy forms tenacious oxide films that reduce surface oxidation at temperatures of 1150 °C. The third alloy, 35Cr-45Ni MA, can be used up to 1150 °C and possess good high temperature strength and carburisation resistance. This micro-alloy offers improved aged ductility and resistance to metal dusting. It is quite suitable for components operating in the hot zones of pyrolysis coils and components of reformer outlet manifolds.

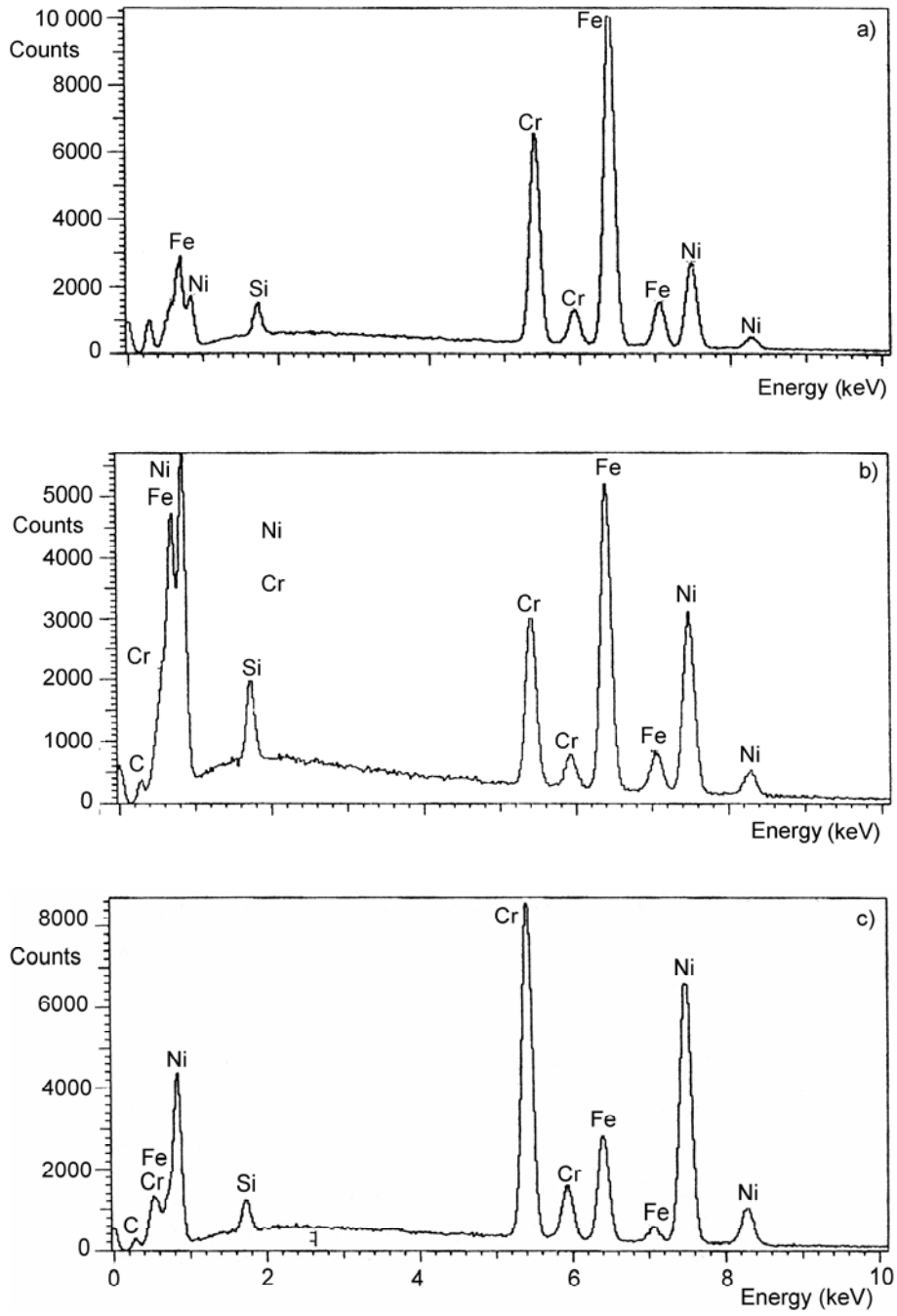

Fig. 1. Energy dispersive X-ray spectra derived from an uncarburised austenite region for verifying the furnace tube material: a) sample No. 2, b) sample No. 5, c) sample No. 8

3.3. Microstructure of furnace tube materials Nos. 1 and 2

A typical optical macrograph of a tube cross-section obtained from sample No. 1 is shown in Figure 2. The carburised zone was about 8 mm in depth. The average carburised depth in samples No. 1 and 2 was observed to be 22% of the tube wall thickness.

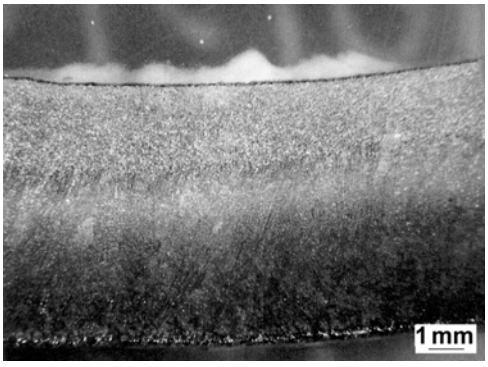

Fig. 2. Optical macrograph of a tube cross-section obtained from sample No. 1 showing the carburised region

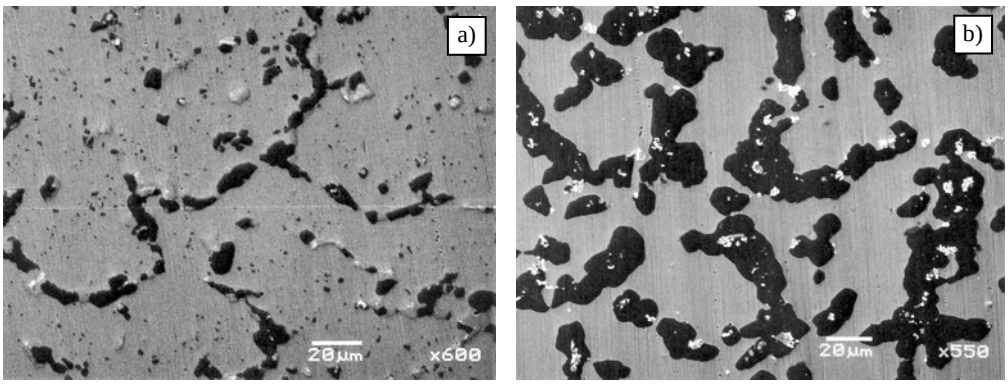

Fig. 3. Secondary electron SEM image obtained from (a) uncarburised and (b) carburised regions of sample No. 1

The microstructure of the uncarburised region is shown in a secondary electron SEM image in Figure 3a. The tube material consisted of relatively large equiaxed grains with precipitation at the grain boundaries. Energy dispersive X-ray spectroscopy revealed that the matrix was comprised of austenite (Fe–Cr–Ni solid solution) and that the grain boundary constituted a Cr-rich carbide. The austenite matrix also revealed the presence of coarse and fine particles of Cr-rich carbides. The microstructure of the carburised region for the same sample is shown in Figure 3b. It can be observed that the Cr-rich carbide precipitates present within the austenite grains are coarser in size compared to those in the uncarburised region.

3.4. Microstructure of furnace tube materials Nos. 3–6

Figure 4 shows the optical macrograph of a tube cross-section from this group of tubes (Nos. 3–6). It can be seen that more than 50% of the wall thickness exhibited signs of carburisation.

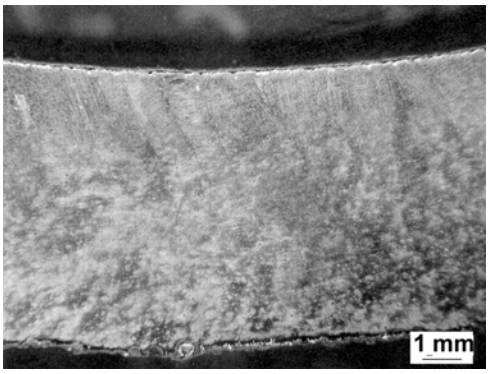

Fig. 4. Optical macrograph of a tube cross-section from sample No. 5 showing the carburised region

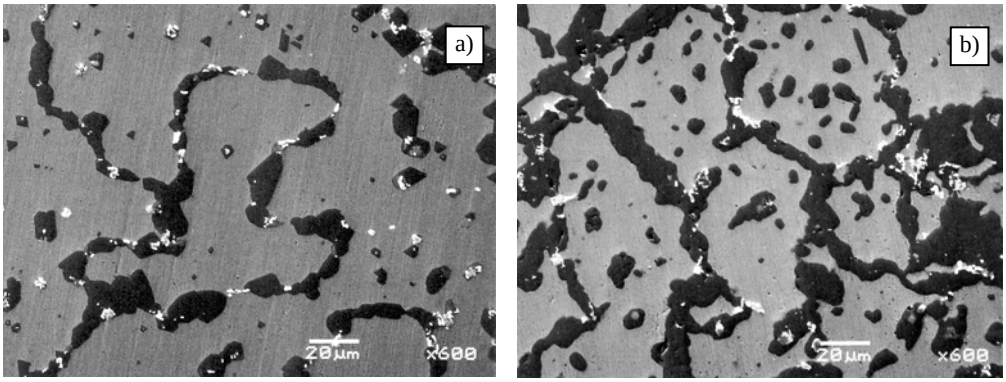

Fig. 5. Secondary electron SEM image obtained from uncarburised (a) and carburised (b) regions of tube sample No. 5

A typical microstructure obtained from an uncarburised region of tube sample No. 5 is shown in the secondary electron SEM image in Figure 5a. Compared to the uncarburised region of tube material No. 1 (see Figure 3a), the carbide precipitation appears relatively coarse both at the austenite grain boundaries and within the matrix itself. This is confirmed by the EDS analysis in which the Cr concentration was determined to be as low as 13 wt. % at various regions within the austenite. The depletion of Cr within the matrix indicates the tendency of Cr to diffuse and form Cr-rich carbides at the austenite grain boundaries and/or coarsen pre-existing carbides within the austenite. The diffusion of Cr is enhanced at elevated temperatures. The higher the temperature, the greater the carburised zone and the coarser the carbide precipitates.

The carburised region from the same sample shows a high degree of carbide precipitation at the grain boundaries and blocky carbide particles in the matrix as shown

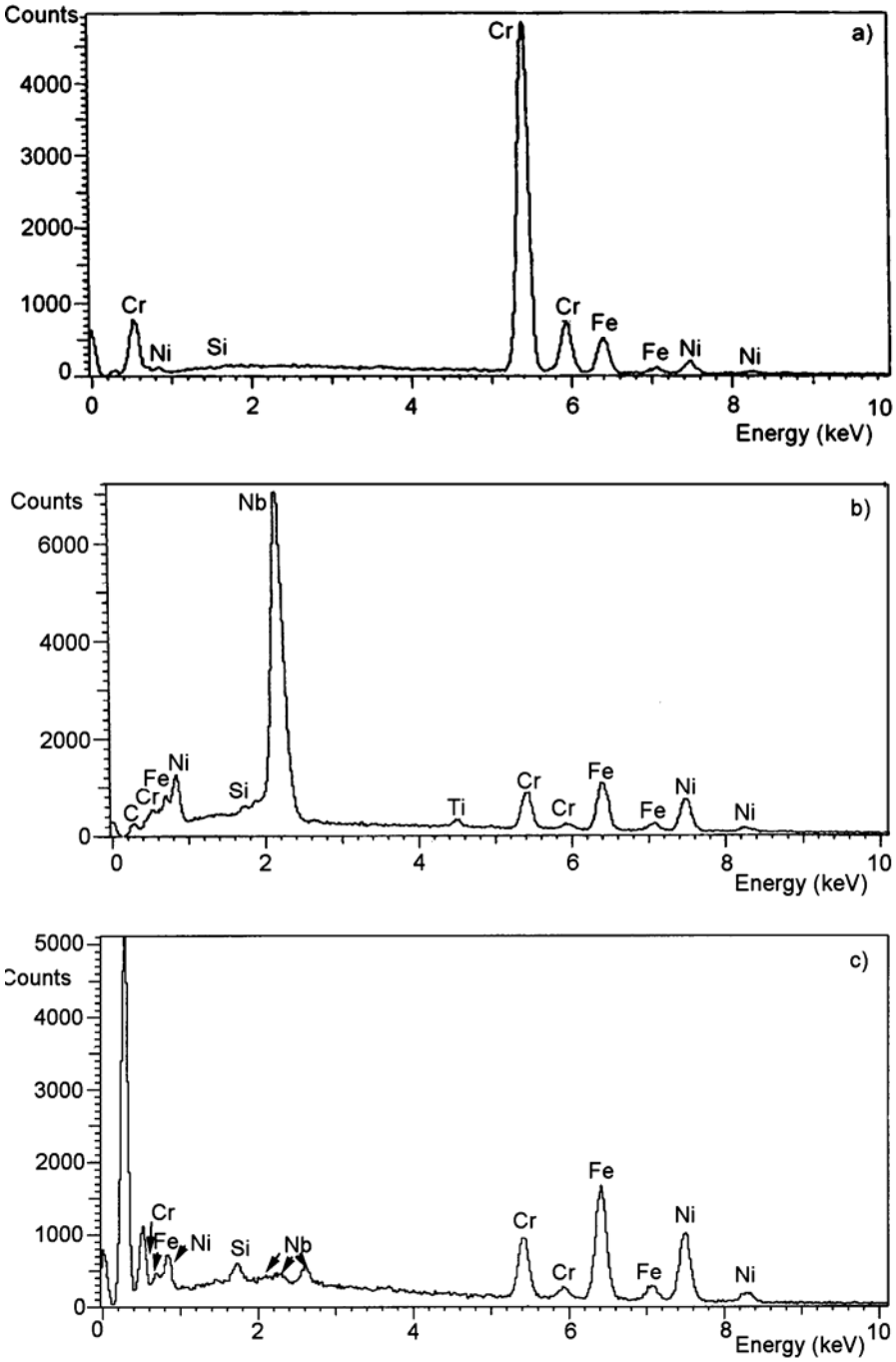

Fig. 6. Energy dispersive X-ray spectra obtained from grain boundary precipitates exhibiting Cr enrichment (a), white precipitates exhibiting Nb enrichment (b), and a carburised region near the tube inner surface (c)

by the SEM image in Figure 5b. The grain boundary precipitate predominantly comprises Cr, as shown by the EDS spectrum in Figure 6a, and is present in the form of a continuous lattice. The white precipitates adjacent to the grain boundaries are Nb-rich, as shown by the EDS spectrum in Figure 6b.

Relatively small additions of Nb to the resistant castings can increase their resistance to thermal shock. Furthermore, Nb acts as a carbide stabilizer by forming MC-type carbides, which prevent massive carbide precipitation at the grain boundaries. The presence of Nb was not detected during material verification by SEM/EDS, probably due to its low concentration within the exposed tube alloy matrix.

Table 2. Chemical composition (wt. %) of a carburised region of HP25-35 alloy

Element	Content (wt. %)
C	61.10
Si	0.83
Fe	16.74
Ni	14.34
Cr	6.79
Nb	0.22

EDS analysis of the carburised region near the inner tube surface (Fig. 6c) showed high C content; the quantified results are summarized in Table 2. Massive carbide precipitation at the austenite grain boundaries (forming a continuous lattice) and the presence of carbides as coarse blocky particles within the matrix indicate the exposure of the furnace tubes to an excessively high temperature that leads to heavy carburisation.

3.5. Microstructure of furnace tube materials Nos. 7–9

Optical and SEM micrographs of the cross-section of tube No. 9 are shown in Figures 7a, b, respectively. The carburised region was approximately 26% of the wall

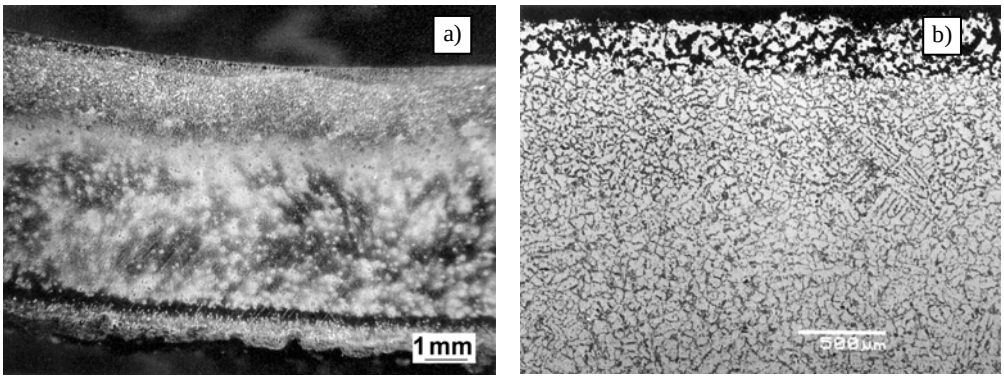

Fig. 7. Optical (a) and SEM (b) micrographs of the cross-section of tube No. 9 showing a carburised region

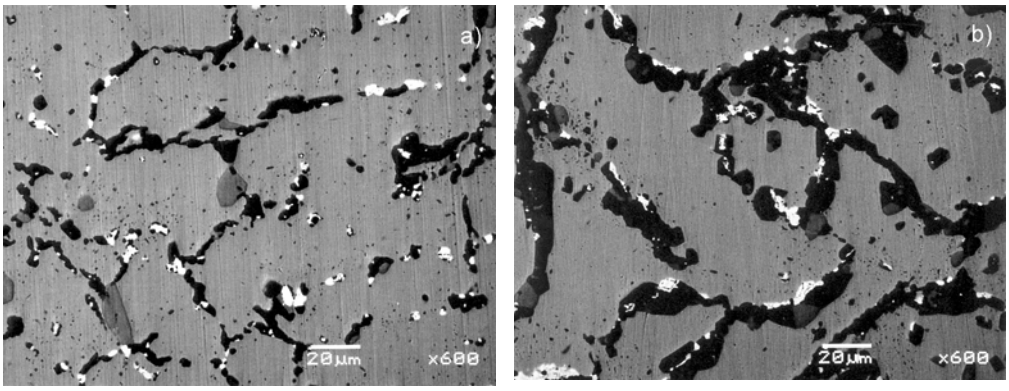

Fig. 8. Secondary electron SEM image obtained from uncarburised (a) and carburised (b) regions of tube sample No. 8

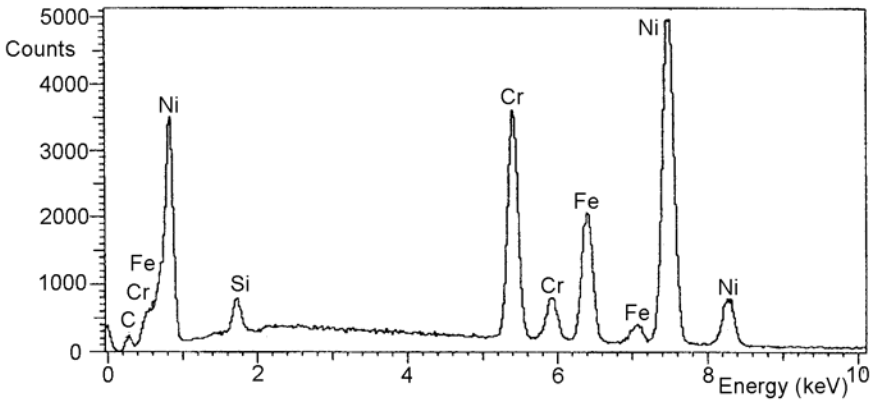

Fig. 9. Energy dispersive X-ray spectrum obtained from light grey precipitates, showing a large peak for Ni

thickness in these samples. Typical microstructures obtained from the uncarburised and carburised regions of the furnace tube material (Nos. 7–9) are shown in Figures. 8a, b, respectively. The microstructures comprised dark Cr-rich and white Nb-rich precipitates, along with greyish precipitates comparatively richer in Ni as shown by the EDS spectrum in Figure 9 and chemical composition in Table 3.

Table 3. Chemical composition of light grey precipitates from sample No. 8

Element	Content (wt. %)
Ni	63.1
Cr	19.8
Si	1.7
Fe	15.4

3.6. Analysis of the scale formed on the furnace tube material (Nos. 1–9)

A typical morphology of the scale formed at the internal surface of the furnace tubes is shown in the backscattered electron SEM image in Figures 10, 11. The scale was discontinuous and broken, thus providing minimal protection to the underlying alloy from diffusing species. The X-ray map and various EDS spectra obtained from the region (Fig. 11) revealed that the oxide formed at the surface was Cr-rich, while Fe and Ni could also be detected in the scale. In addition, Si and to some extent Cr-rich oxides were detected at the austenite grain boundaries just below the alloy surface. The Cr content of the austenite grains in this region was as low as 4.2 wt. %, which is inadequate to sustain a continuous protective Cr_2O_3 scale.

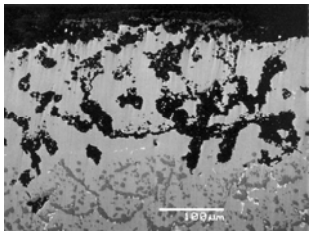

Fig. 10. Backscattered electron SEM image showing a typical morphology of scale formed at the internal surface of the tube material

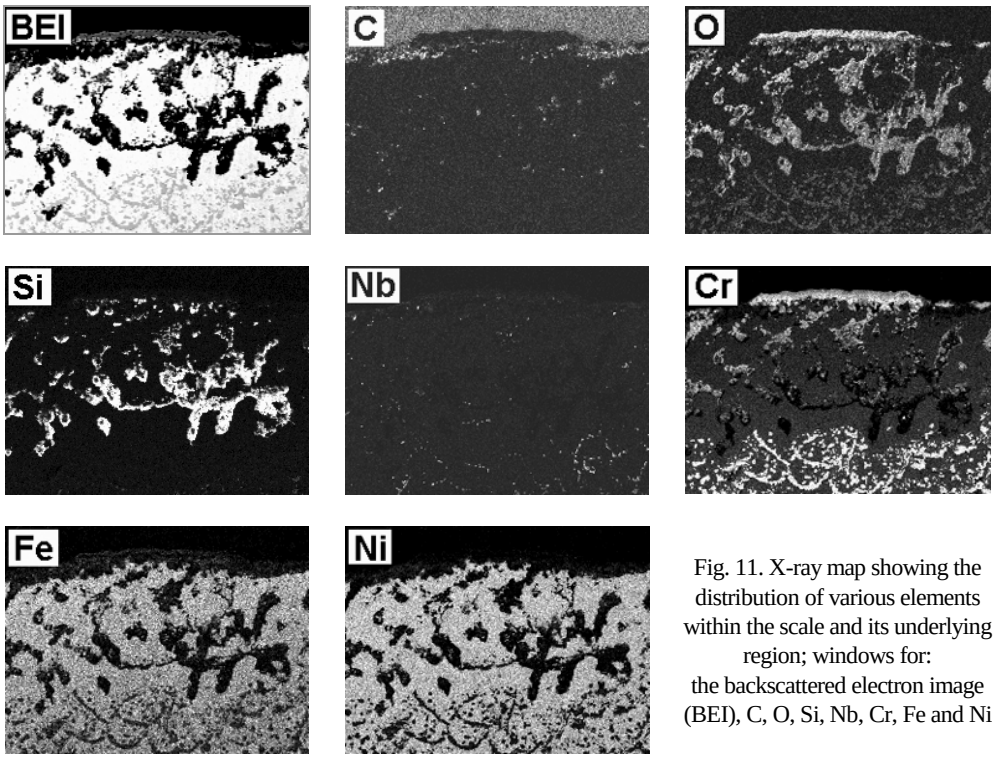

Fig. 11. X-ray map showing the distribution of various elements within the scale and its underlying region; windows for: the backscattered electron image (BEI), C, O, Si, Nb, Cr, Fe and Ni

Based on the above observations, it can be concluded that the alloys were incapable of developing a protective oxide scale. This could partly be due to the relatively low oxygen potential of environments typically encountered in ethylene production. The presence of a protective oxide scale can impede C diffusion into the alloy and play an important role in reducing the extent of carburisation. Earlier studies of carburisation have shown that in severely carburising environments, where the carbon activity reaches 1, Cr_2O_3-forming alloys develop surface carbide scales rather than oxide scales [3]. It is evident from the above results that the oxygen potential of the environment promoted the formation of an oxide scale. The scale was not protective, however, as indicated by the presence of voids, which permitted the penetration of carbon into the alloy substrate.

3.7. Microhardness measurements

At the inner surface of the tube, where carburisation was most severe, the average hardness was found to be HV 316 corresponding to HRC 32. Towards the outer surface, however, the average hardness was reduced to HV 216 corresponding to HB 206. In as-cast conditions, the room temperature hardness of these alloys is typically HB 171. Two factors can contribute to the observed hardening, namely a) carburisation and b) thermal aging. Hardening due to carburisation is expected to predominate near the inner surface of the tube. In contrast, the effect of thermal aging should progressively increase with depth from the inner surface. Increased hardness at the carburised zone can be attributed to the high degree of carbide precipitation and also to C pickup due to the carburising environment. Hardness measurements, combined with microstructural observations, suggest that carburisation led to the formation of a surface hardened layer of reduced ductility. The formation of this layer further confirms the inability of the alloy to form a continuous protective oxide scale at its surface.

4. Discussion

Carburisation occurs when C from the environment combines at elevated temperatures primarily with Cr and other carbide formers (Nb, W, Mo, Ti, etc.) present in the alloy. The carbides may be quite complex and form within the grains and along grain boundaries. They are hard and brittle. The overall effect is a drastic reduction of ductility at elevated temperatures, a reduction of oxidation resistance, and an adverse affect on creep strength. Carburisation is common in ethylene cracking furnaces due to the presence of high tube metal temperatures – up to 1150 °C (which is the practical upper limit for most heat resistant alloys) – and high carbon potentials associated with the hydrocarbon feedstock. The carburisation of furnace tubes is unpredictable and non-uniform in nature.

The typical microstructure of heat-resisting austenitic casting steels consists of an austenite matrix and carbide precipitates. The use of varying contents of Cr and Ni in these alloys allows properties such as, resistance to carburisation, and hot gas corrosion to be controlled strength at elevated temperatures. Nickel imparts the alloy with an increased resistance to carburisation, thermal shock, and thermal fatigue, while chromium provides increased corrosion and oxidation resistance [4]. Fine dispersion of carbides in the austenitic matrix increases high temperature strength to a considerable extent. Rapid cooling from a temperature near the melting point results in the supersaturation of C. Subsequent reheating (e.g. during service) results in carbide precipitation. The lower the reheating temperature, the finer the precipitated carbides. Finer dispersion of carbides increases the creep strength of the alloy. Exposure to high temperatures, however, results in the coarsening, agglomeration, and spheroidising of carbides, thus reducing their effectiveness as a source of strength. In addition, slow cooling from a high temperature results in carbide precipitation at austenite grain boundaries. A continuous lattice of carbides at the grain boundaries is undesirable, since they embrittle the alloy. The size of carbides can thus be useful in indicating whether the alloy has been exposed to excessive temperatures during service.

All the furnace tubes examined in this study exhibited carburisation. The average depth of the carburised zones in furnace tubes Nos. 3–6 was 58% of the total wall thickness, as compared to 22% for tubes Nos. 1–2 and 26% for tubes Nos. 7–9. Moreover, visual examination also revealed that tubes Nos. 3–6 were clearly sagged, indicating significant plastic deformation during service. Clearly, tubes Nos. 3–6 exhibited the most severe degradation amongst the studied samples. This was also confirmed by SEM/EDS examination, in which the microstructures of tubes Nos. 3–6 exhibited relatively coarse blocky carbides within the austenite matrix and a continuous carbide lattice at the grain boundaries. Massive precipitation of carbide phases is typical of carburisation [5, 6]. These observations suggest that the alloy had been exposed to an excessively high temperature during service. The hardness of the carburised zone was also found to be higher in tubes Nos. 3–6 as compared to the other tube materials, indicating a higher precipitation and C pickup by the alloy. The deposition of coke on the inner pipe wall also promotes C diffusion and the precipitation of secondary carbides within the alloy. As demonstrated earlier under the operating conditions, the tube alloy develops a non-protective surface oxide scale. Carbon deposited on the surface can readily penetrate the oxide scale into the alloy substrate, where it reacts with carbide-forming elements, particularly Cr, to form the observed Cr-rich carbides.

5. Conclusions

Experimental data shows that all the tube materials had undergone carburisation due to exposure to excessively high temperatures during service. Carburisation was

most severe in tubes Nos. 3–6, indicating that these could have been overheated for relatively longer periods during service compared to others.

The temperature of the furnace should be controlled closely, in order to avoid over-heating during ethylene production and decoking.

Acknowledgements

The authors wish to acknowledge the support of the Research Institute of King Fahd University of Petroleum and Minerals, Dhahran, Saudi Arabia.

References

[1] BLACKBURN J., [in:] *Carburization in High Temperature Process Plant Materials*, Colloquium Proceedings Coordinated by J. Norton, Commission of the European Communities, Luxembourg, Report No. EUR 7773, 1981, 7.
[2] NACE Standard TM 0498-98-Item No. 21235.
[3] LAI G. Y., [in:] *High Temperature Corrosion in Energy Systems*, M. F. Rothman (Ed.), TMS-AIME, Warrendale, Pennsylvania, 1985, 551.
[4] *ASM Metals Handbook, Properties and selection of metals*, Vol. 1, 8th Edition, 1977.
[5] TAWANCY H.M., ABBAS N.M., J. Mater. Sci., 26 (1992), 1061.
[6] SCHNAAS A., GRABKE H.J., Oxidation of Metals, 12 (1978), 387.

Received 16 May 2005
Revised 24 July 2005